Size dependence of switching field of magnetic tunnel junctions down to 50 nm scale

H. Kubota,[a] Y. Ando, and T. Miyazaki
Department of Applied Physics, Graduate School of Engineering, Tohoku University, Sendai 980-8579, Japan

G. Reiss, H. Brückl, and W. Schepper
Department of Physics, University of Bielefeld, P.O. Box 100131, 33501 Bielefeld, Germany

J. Wecker and G. Gieres
Siemens AG, Zentrale Technik ZT MFI, P.O. Box 3220, 91050 Erlangen, Germany

(Received 3 December 2002; accepted 8 May 2003)

Tunnel magnetoresistance curves were measured in very small tunnel junctions from scales of 1 μm to 50 nm using conductive atomic force microscopy. The junction arrays were prepared by a simple fabrication process using electron beam lithography. In large size junctions, the minor loops shifted in the negative field direction corresponding to ferromagnetic coupling between free and pinned layers. With decreasing size, the shift changed to the positive field direction corresponding to antiparallel coupling. The dependence of the shift was quantitatively explained by a model taking account of both Néel-type and dipole coupling. The minor loops showed asymmetric shape depending on field sweep directions. © *2003 American Institute of Physics.*
[DOI: 10.1063/1.1588357]

I. INTRODUCTION

Magnetic tunnel junctions (MTJs) have been intensively studied from both fundamental[1,2] and practical points of view.[3,4] MTJs have many properties which make advanced microelectronic devices such as magnetic read head or magnetic random access memory (MRAM) promising. The magnetization process of MTJs microstructured into submicron scale, features prominently in these devices. For MRAM application, the magnetization switching properties of soft magnetic thin film islands or MTJs have been well studied at a scale of a few hundred nanometers.[5–8] The junction size could be decreased to 100 nm or less at the MRAMs with a capacity of more than 1 Gbit. However, the magnetization process of such small MTJs has not been studied, because of difficulties in their fabrication and characterization. In the fabrication process, the size limit is dominated by not only the resolution limit of lithography but also the accuracy of pattern alignment. In our standard fabrication process, it is very difficult to make a contact hole to the surface of a top electrode through a thick insulating layer in a submicron junction. If a very small metal electrode through which current flows into the junction, can be attached to the top of the junction, the second problem can be solved. For this purpose, we developed a simple method using conductive atomic force microscopy (*c*-AFM).[9] In principle, this method makes it possible to characterize very small junctions down to the resolution limit of the lithographic process. In this study, the measurement method using *c*-AFM is applied to the investigation of the switching properties of free layers in MTJs with junction areas between 1 μm^2 and 2.5×10^{-3} μm^2. The size dependence of the switching properties are discussed.

II. EXPERIMENTAL PROCEDURE

A multilayer with a stacking sequence of Si/SiO_2/Ta (5 nm)/Cu (30 nm)/CoFe (1.5 nm)/Ru (0.9 nm)/CoFe (2.2 nm)/Al (1.5 nm)–O/NiFe (6 nm)/Ta (5 nm)/Au (30 nm) was prepared using sputtering and plasma oxidation.[10] Electron beam lithography and Ar ion etching were used to define the patterns ranging from 30 nm to 1 μm and with aspect ratio from 1:1 to 1:7. Etched depth was controlled using secondary ion mass spectroscopy (SIMS). Etching was stopped just before SIMS signal of Al disappeared. Surface of the bottom electrode CoFe was probably etched because spatial distribution of etching rate was rather large. Figure 1 shows a schematic illustration of the measurement system. A commercial atomic force microscope (Thermo microscope) was customized: An $X-Y$ sample positioner with nonmagnetic material was fixed on a stage made of nonmagnetic stainless steel and aluminum. An AFM scanner and the sample stage with the $X-Y$ positioner were located between the coils. The whole measurement system was mounted on a vibration isolator. Diamond coated tips with a high force constant were used. Currents flowing through the tip and junctions were measured using a lock-in technique with a constant applied voltage. An AFM contact mode image and a current image were obtained simultaneously. Due to the restricted field range of the magnetic coils, only minor loops were measured.

III. RESULTS AND DISCUSSION

A. Measurement technique

Figures 2(a) and 2(b) show the AFM contact mode image and the corresponding current image for a part of the

[a]Author to whom correspondence should be addressed; electronic mail: kubota@mlab.apph.tohoku.ac.jp

 © 2003 American Institute of Physics

Downloaded 09 Dec 2008 to 130.34.135.83. Redistribution subject to AIP license or copyright; see http://jap.aip.org/jap/copyright.jsp

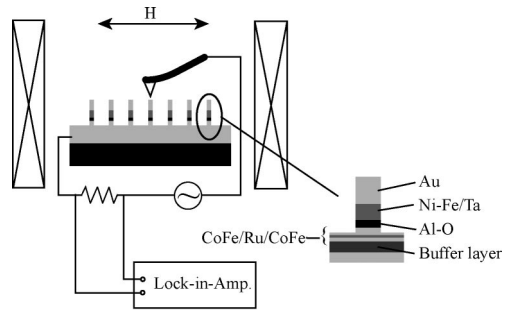

FIG. 1. Schematic illustration of the measurement setup for tunnel magnetoresistance using conductive atomic force microscopy.

junction arrays, respectively. The line profile of the height and the current between points A and B are shown in Figs. 2(c) and 2(d), respectively. The junctions shown in the figure had a constant width of 500 nm, while their lengths varied from 500 to 1500 nm. Most of the junctions showed regularly rectangular shapes that agreed well with the design. The heights of the junctions were almost identical except for the junctions in the left column and the bottom row. The line profile shown in Fig. 2(c) shows this fact more clearly. The first left junction is shorter than other junctions. Figure 2(b) shows that the currents flowed only when the AFM tip was on top of the junction pattern. It is obvious that large size junctions are brighter than smaller ones. The elements appearing bright had high conductance while the dark ones had low conductance. The current values are proportional to junction area as shown in the line profile. The left junction in Fig. 2(d) showed lower currents, corresponding to the lower height. Some other junctions located near the left and bottom corner in Fig. 2(b) also showed lower heights and very low currents. The top Au layers of these junctions were possibly removed in the resist stripping process or during the measurement in which the AFM tip was scanned to find out the junction array. The loss of the Au layer on the junction surface results in poor electrical contact between the tip and the junction surface. Except for damaged junctions the resistance$\times$area product agreed well with the mean value of 2 MΩ μm^2 measured on 50 μm$\times$50 μm large MTJs. For

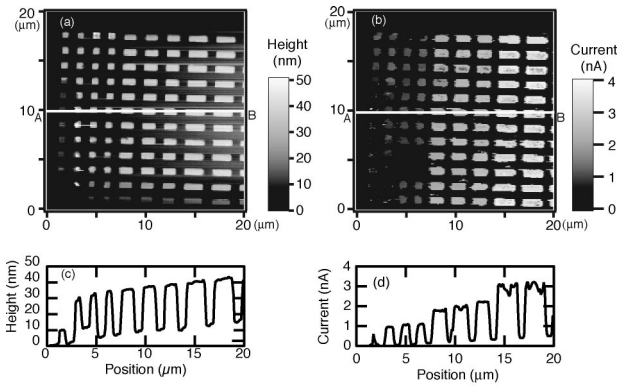

FIG. 2. (a) AFM image and (b) current image of a tunnel junction array. Line profiles along the lines between points A and B are also shown in (c) and (d). The width of the junctions were constant at 500 nm, while the length varied from 500 to 1500 nm.

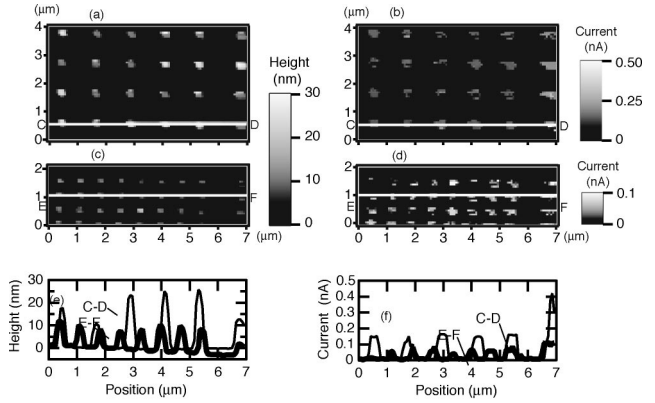

FIG. 3. (a) and (c) AFM images and (b) and (d) current images of a tunnel junction array. Profiles along the lines C–D and E–F are shown in (e) and (f). The junctions were 100×200 nm^2 in (a) and (b), and 30×210 nm^2 in (c) and (d).

example, elements with an area of 0.5 μm$\times$1.5 μm had a resistance of about 2.4 MΩ. It should be noted that the apparent sizes of the junctions in the current image were slightly larger than those in the topographic contact mode image. These differences were due to the tip radius: the current started to flow as soon as the side surface of the tip touched the Au layer. Thus, the bright area in the current image is equal to $(W+2r)\times(L+2r)$, where *W*, *L*, and *r* correspond to junction width, length and tip radius, respectively. From scanning electron microscopy images, *r* can be estimated to be around 150 nm, which is in the same range as obtained from the comparison of the topographic and current images. Due to the irregular shape of the diamond coated tips, however, an exact evaluation of *r* seems not to be meaningful.

Figures 3(a)–3(d) show the AFM contact mode images and the corresponding current images for smaller junctions. The junction sizes were 100 nm$\times$200 nm [Figs. 3(a) and 3(b)] and 30 nm$\times$210 nm [Figs. 3(c) and 3(d)]. The surfaces in Figs. 3(a) and 3(c) appear less well resolved than in Fig. 2(a) because fewer lines were scanned and fewer points in the lines. The current images [Figs. 3(b) and 3(d)] were much rougher than Fig. 2(b). The low resolution scan was also responsible, but poor electrical contact due to the loss of the Au layer on the junction surface or a damaged tip surface could be another reason. The line profiles of the height between the line C–D and the line E–F are shown in Fig. 3(e). The profiles appear as triangular peaks rather than trapezoidal shape. This was due to the tip radius effect as already described. The height decreased with decreasing size. After development, resist layers defining smaller junction areas would be thinner than those for larger junction areas. Then, the Au layer on the smaller junctions are partially etched during the Ar ion etching process and/or the oxygen ashing process. The line profiles of the current image were trapezoidal. The current decreased with decreasing junction size. In the smallest junctions, corresponding to the line E–F, the variation of current values through the junctions were relatively large, because the absolute values of the currents were very small and the electrical contact was not so stable in the

Downloaded 09 Dec 2008 to 130.34.135.83. Redistribution subject to AIP license or copyright; see http://jap.aip.org/jap/copyright.jsp

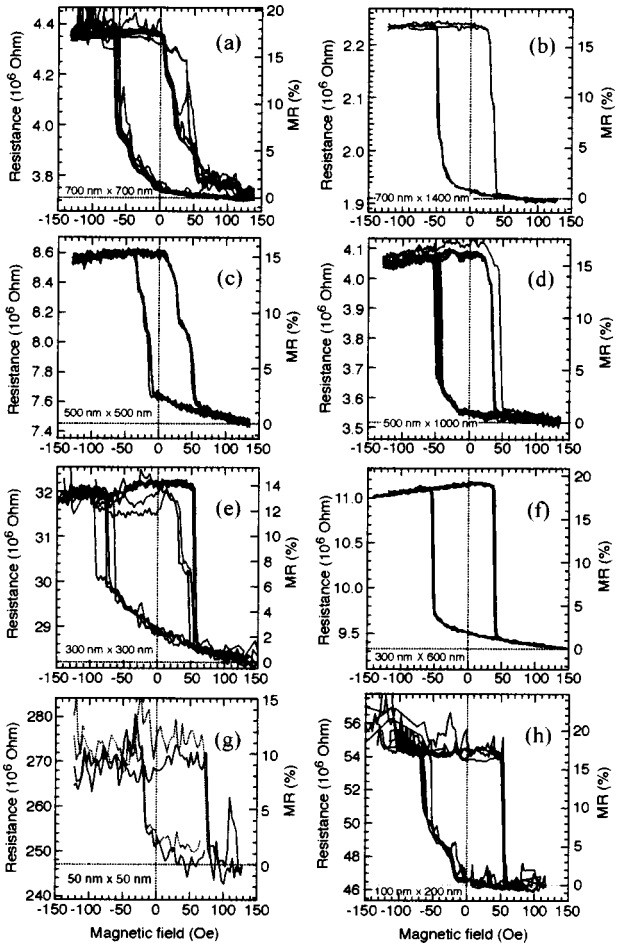

FIG. 4. Typical magnetoresitance curves of MTJs measured using conductive AFM. Junction width varied between 50 and 700 nm. The MTJs in the left column had an aspect ratio of 1, while those in the left column more than 2.

scan. It was, however, still possible to distinguish between working and damaged MTJs. In conclusion, conductive AFM method is very useful for characterizing very small MTJs. The advantage of this technique is the high lateral resolution and reduction of the junction size limit to several tens of nanometers. Disadvantages are an unstable contact depending on the tip condition, the sample drift, and a high contact resistance of the order of $10^2-10^3\ \Omega$. Particularly for small MTJs with a junction resistance of the order of $10^6\ \Omega$ or more, however, the last point does not cause deterioration in the measurement results.

B. Tunneling magnetoresistance measurement

In order to measure magnetoresistance hysteresis loops on individual junctions, the AFM tip was positioned on the selected junction and the currents were measured during several sweeps of the magnetic fields. Figures 4(a)–4(h) are typical minor loops measured on the junctions with aspect ratio (W:L) of 1:1 and 1:2. The junction width (W) is between 700 and 50 nm. Magnetic switching of the soft NiFe layer between magnetizations parallel and antiparallel to the upper CoFe layer was clearly observed in every junction measured. The magnetizations of the soft NiFe and the CoFe

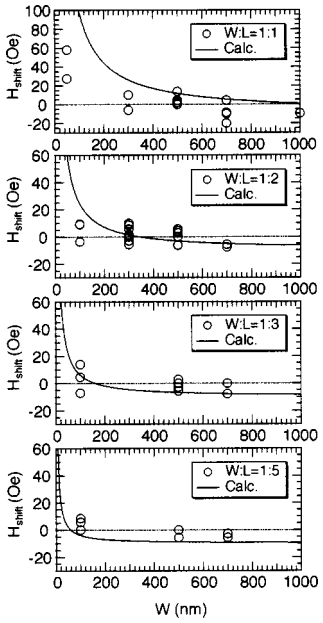

FIG. 5. Junction width dependence of loop shift (H_{shift}). H_{shift} is defined as the center shift of the minor loop.

layers were saturated by applying a large positive field prior to the minor loop measurement. According to previous report, magnetization of a thicker magnetic layer in artificial antiferromagnet would remain parallel to the direction of magnetic field.[11] The junctions with higher aspect ratio (W:$L=1:2$) showed relatively symmetric and smooth switching. The switching fields increased from 40 to 60 Oe with decreasing W. The signals at zero field were close to the values at the maximum fields. The remanent magnetizations of NiFe free layers at high-resistance states would be almost identical to the saturation values. The remanent magnetizations at low-resistance states were estimated to be 70%–90% of the saturation values. This reduced remanent magnetization will be discussed in part C. In square junctions, we frequently observed steps in the switching process. The loop shapes were asymmetric: when magnetic fields were swept from the positive side to the negative side, the resistance increased gradually. This resulted in a decrease of signal difference between the two remanent states. The center of the minor loops was shifted to the negative side in most of junctions; however, it shifted to the positive side remarkably in Fig. 4(g), which shows the loops with the smallest junction measured in this experiment.

Figure 5 shows the dependence of the loop shift (H_{shift}) on junction width (W) for various aspect ratios. The circles and solid lines represent experimental data and calculations, respectively. The experimentally determined H_{shift} increased slightly with decreasing W in every aspect ratio. The trend is most pronounced in the square junction: the loop shift changed from negative to positive fields. The loop shift is a result of competition between ferromagnetic Néel coupling through the rough interface[12] and magnetostatic coupling at the edges of the magnetic layers.[6] The ferromagnetic Néel coupling, shifts the loop to the negative field and the magnetostatic coupling to the positive field in this experiment,

Downloaded 09 Dec 2008 to 130.34.135.83. Redistribution subject to AIP license or copyright; see http://jap.aip.org/jap/copyright.jsp

because magnetizations of the soft NiFe and the bottom surface CoFe were aligned parallel at large positive fields. Taking these two effects into account, the total loop shift (H_{shift}), which is sum of the ferromagnetic coupling (H_D) and the antiferromagnetic coupling (H_N), was calculated analytically. H_D is expressed as follows:

$$H_D = \frac{2M_S tW}{\mu_0 (L^2+4x^2)\sqrt{1+\dfrac{(W^2+4x^2)}{L^2}}},$$

where M_S, t, and x are the magnetization and the thickness of the bottom surface layer, and the thickness of the insulator, respectively.[9] It was assumed that the bottom hard layer was homogeneously magnetized and completely etched. Thus, the equation corresponds to the maximum value expected experimentally. H_N can be evaluated from the experiments on very large size junctions. A junction with an area of 50 μm$\times$50 μm fabricated using the conventional lithographic process showed a loop shift of about -10 Oe. This value of H_N was comparable with those of previous reports.[6] The calculated values of H_{shift} for various aspect ratios are shown by solid lines in Figs. 5(a)–5(d). The calculated values were negatively constant (-10 Oe) at large W, which means H_D is negligibly small. The values increased rapidly when W was less than the critical values and increased with decreasing the aspect ratio. The experimental data scattered around the calculated values. The magnitudes of the calculated loop shift agreed only roughly with the experiments. This is due to the variation of switching characteristics among the MTJs and due to the simple assumption of a homogeneous magnetization of the hard layer. Moreover, the CoFe layer at the bottom electrode surface was probably etched in the Ar ion etching process. Thus, a variation of etched depth could also result in a variation of stray field strength. When the bottom CoFe/Ru/CoFe artificial antiferromagnet layer was completely etched, stray fields from both CoFe layers would be canceled out each other, resulting in smaller H_{shift}.[13]

Figures 6(a)–6(d) show the dependence of the coercivity (H_C) on W. The value of H_C was determined as half the width of the minor loop. In larger aspect ratio junctions, H_C increased significantly with decreasing W. This increase agreed with the previous result, where H_C was inversely proportional to W. The elongated shape of the element induced magnetic shape anisotropy, which stabilized the magnetization aligned parallel to the easy axis. The tendency became weak with decreasing the aspect ratio. In the junctions with an aspect ratio of 1:1, H_C did not show an increase at $W \leqslant 700$ nm. Some steps in the magnetoresistance (MR) loops in the low aspect ratio junctions suggested complex motions of domain walls of the free layers in the magnetization process.

As mentioned earlier, there are some common features of the MR loops, e.g., loop shift and asymmetric shape between the two field sweep directions. In Ref. 14, magnetization configurations were simulated by micromagnetic calculation, where Zeeman energy, uniaxial anisotropy energy, exchange energy, and dipole coupling energy were taken into account. Figure 6 in Ref. 14 corresponded to magnetization configurations of a free layer in the MTJ with junction area of 50 nm$\times$50 nm. The shape of the magnetoresistance curve reproduced agreed with that of the experimental result on the same size junction. In all the field ranges, no distinct domain wall was observed in the simulation. Magnetic moments at the center of the square were aligned parallel to the field direction but those at the four corners were bent. The remanent state had the magnetization configuration like the letter "*X*," which was different from C-shape or S-shape configurations well known in rectangular junctions.[15] This seems very reasonable if demagnetization effects are taken into account. Magnetization configurations simulated during sharp transitions in Ref. 14 showed complicated structures. If such intermediate states were stable in a certain field range, it would lead to steps in the MR loop as observed in Figs. 4(a)–4(e). In the junction with area of 50 nm$\times$50 nm, the lateral size of the free layer was rather small, so that, large angles between neighboring moments in the intermediate states could increase the exchange energy. Since the intermediate states were energetically unstable, sharp transitions were realized.

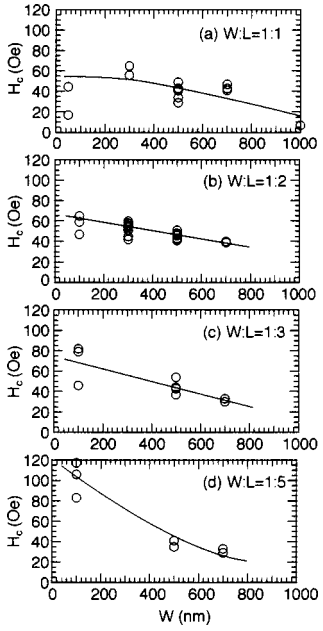

FIG. 6. Junction width dependence of coercive field (H_c). H_c defined as half the width of the minor loop.

IV. SUMMARY

Submicron sized rectangular MTJs with various aspect ratios were fabricated using an electron beam lithographic technique. Conductive AFM was applied to resistance and magnetoresistance measurement for the MTJs. Minor hysteresis loops of the free layers gave magnetoresistance curves showing both loop shift and asymmetric shape. The loop shift was due to dipole coupling between the free layer and the bottom surface layer. The increase in the shift with decreasing junction width was quantitatively explained by the analytical model that took account of the dipole field from the bottom surface. The smallest MTJ with junction area of

Downloaded 09 Dec 2008 to 130.34.135.83. Redistribution subject to AIP license or copyright; see http://jap.aip.org/jap/copyright.jsp

50 nm×50 nm showed sharp switching. This would suggest that MTJs as small as 50 nm can be applied to memory cells in ultrahigh density MRAM.

ACKNOWLEDGMENTS

This work was partially supported by a Grant-in-Aid for scientific research by the Ministry for Education, Science, Sport, and Culture (Japan), and the IT-program of RR2002 from mext. One of the authors, H.K. would like to thank Dr. K. Rott, Dr. T. Kaps, A. Thomas, H. Koop, D. Meyners, M. Justus, Dr. Kleinberg, Dr. A. Hütten, and other members of the Bielefeld group for technical assistance and useful discussions. He would also like to thank Volker Hagen in University of Hamburg for a kind suggestion about a conductive AFM experiment and tip selection.

[1] T. Miyazaki and N. Tezuka, J. Magn. Magn. Mater. **139**, L231 (1995).
[2] J. S. Moodera, L. R. Kinder, T. M. Wong, and R. Meservey, Phys. Rev. Lett. **74**, 3273 (1995).
[3] S. S. P. Parkin *et al.*, J. Appl. Phys. **85**, 5828 (1999).
[4] S. Tehrani *et al.*, IEEE Trans. Magn. **36**, 2752 (2000).
[5] S. E. Russek, J. O. Oti, and Y. K. Kim, J. Magn. Magn. Mater. **198–199**, 6 (1999).
[6] A. Anguelouch, B. D. Schrag, G. Xiao, Yu Lu, P. L. Trouilloud, R. A. Wanner, W. J. Gallagher, and S. S. P. Parkin, Appl. Phys. Lett. **76**, 622 (2000).
[7] J. Shi, S. Tehrani, and M. R. Scheinfein, Appl. Phys. Lett. **76**, 2588 (2000).
[8] X. Zhu, P. Grütter, V. Metlushko, and B. Ilic, Phys. Rev. B **66**, 024423 (2002).
[9] H. Kubota, G. Reiss, H. Brückl, W. Schepper, J. Wecker, and G. Gieres, Jpn. J. Appl. Phys., Part 2 **41**, L180 (2002).
[10] J. Schmalhorst, H. Brückl, G. Reiss, G. Gieres, and J. Wecker, J. Appl. Phys. **91**, 6617 (2002).
[11] C. Tiusan, T. Dimpoulos, K. Ounadjela, M. Hehn, H. A. M. van den Berg, V. da Costa, and Y. Henry, J. Appl. Phys. **87**, 4676 (2000).
[12] J. C. S. Kools, W. Kula, D. Mauri, and T. Lin, J. Appl. Phys. **85**, 4466 (1999).
[13] Y. Fukumoto and A. Kamijo, Jpn. J. Appl. Phys., Part 2 **41**, L183 (2002).
[14] W. Schepper, H. Kubota, and G. Reiss, in *Nanostructured Magnetic Materials and Their Applications*, Springer Lecture Notes in Physics, Germany Vol. 2593 edited by D. Shi, B. Aktas, L. Pust, and F. Mikailov (Springer, Berlin, 2002), p. 75.
[15] Y. Zheng and J.-G. Zhu, J. Appl. Phys. **81**, 5471 (1997).

Downloaded 09 Dec 2008 to 130.34.135.83. Redistribution subject to AIP license or copyright; see http://jap.aip.org/jap/copyright.jsp